# Optical-absorption spectra of $CsFeCl_3 \cdot 2H_2O$. II. Magnetic field dependence

H. Okada, N. Kojima, T. Ban, and I. Tsujikawa
*Department of Chemistry, Kyoto University, Kyoto 606, Japan*
(Received 9 January 1990; revised manuscript received 23 August 1990)

The quasi-one-dimensional Ising-like antiferromagnet $CsFeCl_3 \cdot 2H_2O$ has been studied by experiments on the absorption spectra under magnetic fields up to 59 kOe. The large reduction of the magnon energy in a cold-magnon sideband is concluded to be caused by the fact that the corresponding excited state of its original exciton line is a singlet state and that the magnetic interaction is one dimensional. The field variation of the spectra around $T_N$ (12.75 K) reveals the behavior of thermally excited magnetic domain walls under the field. In addition, the existence of domain walls induced by magnetic fields is discussed.

## I. INTRODUCTION

$CsFeCl_3 \cdot 2H_2O$ (CFC) is well known as a quasi-one-dimensional Ising-like antiferrimagnet.[1-8] Its one-dimensional chains run along the $a$ axis. On the basis of an effective $S = \frac{1}{2}$ Ising model, the intrachain and the interchain interactions have been estimated to be $J_a/k = -40.4$ K and $(J_b + J_c)/k = -0.71$ K, respectively.[1,8] The Néel temperature is 12.75 K,[6] and the magnetic structure below this temperature is sketched in paper I.[9] The magnetic moments are located in the $ac$ plane at an angle of 15° from the $a$ axis, and their magnitudes along the $a$ and $c$ axes are $g_a S_a = 4.25$ and $g_c S_c = 1.14$, respectively.[1] The chains have weak ferromagnetic moments parallel to the $c$ axis, and these weak moments are ordered antiferromagnetically along the $b$ and $c$ axes without external magnetic field. When the external magnetic field parallel to the $c$ axis is applied at 4.2 K, these weak moments are ordered ferrimagnetically in the 6.5 kOe ($H_{c1}$) to 9.5 kOe ($H_{c2}$) region and are ordered ferromagnetically above 9.5 kOe ($H_{c2}$).[1]

In paper I[9] we investigated the temperature dependence of the absorption spectra of CFC, and in the present paper we investigate the external magnetic field dependence of these spectra. One purpose of the present paper is to clarify the transition mechanisms of the absorption lines of which the assignments have not been obtained in paper I.[9] Moreover, the magnetic properties of excited states and the behavior of domain walls under external magnetic fields are discussed in the present paper.

## II. EXPERIMENTAL PROCEDURE

Magnetic fields up to 29 and 59 kOe were produced by an electromagnet and a Helmholtz-type superconducting magnet, respectively.

The absorption spectra were measured by the following photoelectric or photographic methods. The photoelectric method was used with a tungsten-iodine projection lamp, a Jasco model CT-100 grating spectrometer, and a Hamamatsu photonics model R-376 photomultiplier. The accuracy of this measurement was ±0.007 nm for sharp absorption lines. On the other hand, the photographic method was used with a xenon arc lamp, a spectrograph, and Kodak TRI-X films. This spectrograph has a holographic grating with 1200 lines/mm and 110 mm wide, and the accuracy of this measurement was ±0.002 nm for sharp absorption lines.

In the measurement around $T_N$, the sample was placed in a glass vessel immersed in pumped liquid helium. This sample was cooled by exchange helium gas inserted into the vessel or was heated by an electric heater near the sample. By the control of the electric power of this heater, constant temperatures (about ±1%) could be held from 2 to 20 K. Temperatures were measured with a germanium resistor at zero magnetic field. In the measurement at very low temperatures, the sample was immersed in liquid helium.

## III. SPECTRA AT VERY LOW TEMPERATURES

### A. Experimental results

In the 24 200–24 280-$cm^{-1}$ region and at low temperatures, the absorption spectra of CFC have the fine structures, which vary remarkably with the external magnetic field parallel to the $a$ axis ($\mathbf{H}_0 \| \mathbf{a}$). Figures 1 and 2 show this variation at 1.7 K in the $a$ polarization ($\mathbf{E} \| \mathbf{a}$). The $A0$ line splits into two components, and the energy difference between them is $3.86 \times 10^{-1}$ $cm^{-1}$ $kOe^{-1}$. The $A1$ line also splits into two components, and the energy difference between them is $3.56 \times 10^{-1}$ $cm^{-1}$ $kOe^{-1}$. The $A2$ line does not split and slightly shifts to the lower-energy side.

Figure 3 shows the energy shifts of the $A0$ and $A1$ lines with $\mathbf{H}_0 \| \mathbf{c}$. Below about 10 kOe, they shift intricately to the lower-energy sides, and the magnitude of the shift between zero field and 10 kOe is $-0.5$ $cm^{-1}$ for the $A0$ line and $-1.3$ $cm^{-1}$ for the $A1$ line. Above about 10 kOe, they shift monotonically to the higher-energy sides, and the magnitude of the shift is $4.8 \times 10^{-2}$ $cm^{-1}$ $kOe^{-1}$ for the $A0$ line and $1.9 \times 10^{-1}$ $cm^{-1}$ $kOe^{-1}$ for the $A1$ line. The $A2$ line scarcely shifts with $\mathbf{H}_0 \| \mathbf{c}$.

 

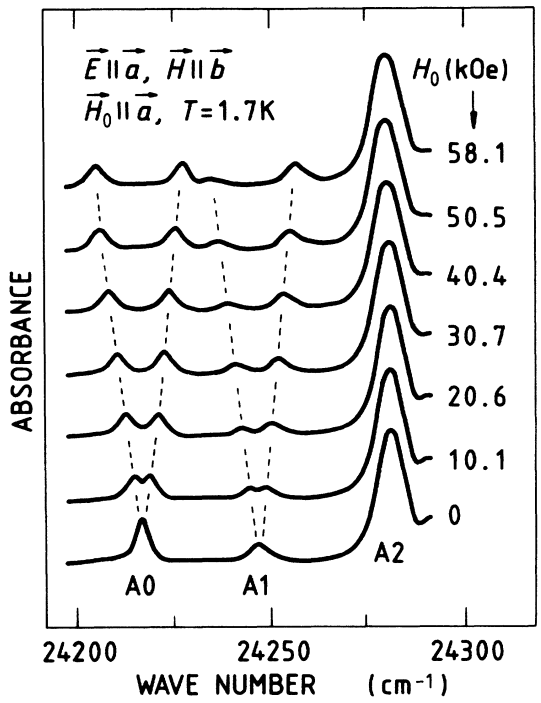


FIG. 1. Absorption spectra in the lowest energy region of the ${}^5T_2(D)\rightarrow\{{}^3T_2(G),{}^3T_1(F),{}^3A_2(F)\}$ transition of $CsFeCl_3\cdot 2H_2O$ at 1.7 K under the external magnetic field along the $a$ axis ($\mathbf{H}_0\|\mathbf{a}$). The symbols **E** and **H** denote the electric and magnetic vectors of the incident light, respectively. The dashed lines are to guide the reader's eye.

With $\mathbf{H}_0\|\mathbf{b}$, the fine structures do not vary.

Figure 4 shows the dependence of the energy shift of the $A0$ line on the direction of the external magnetic field (27.3 kOe). The solid curve is discussed in the next subsection.

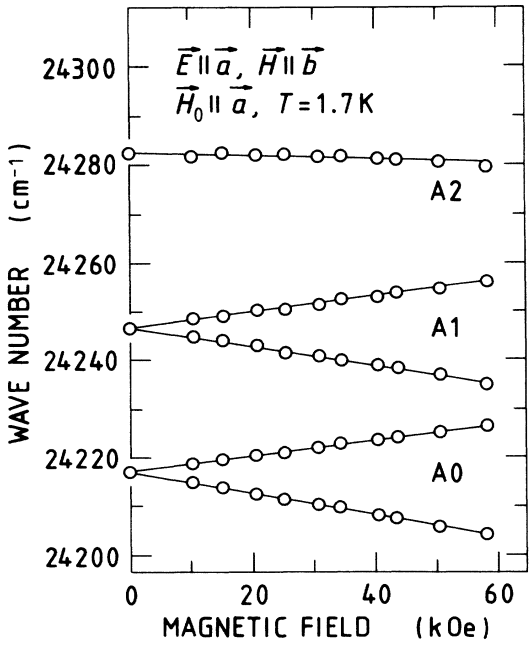


FIG. 2. Energy shifts of the $A0$, $A1$, and $A2$ lines with $\mathbf{H}_0\|\mathbf{a}$ at 1.7 K. The solid lines are a guide for the eye.

### B. Excited state corresponding to the $A0$ line

As mentioned in paper I,[9] the $A0$ line is an exciton line attributed to a spin-forbidden transition. In this subsection, we will reveal the magnetic property of its excited state by examining its energy shift with external magnetic fields.

The energy shift of an exciton line with $\mathbf{H}_0\|\mathbf{i}$ axis ($\mathbf{i}=a,b,c$), expressed by $\delta_i^{ex}$, is described as

$$\delta_i^{ex}=(g_iS_i-g_i^*S_i^*)\mu_BH_0\ , \tag{1}$$

where $g_i$ and $g_i^*$ are the effective $g$ values and $S_i$ and $S_i^*$ the spin components along the $i$ axis in the ground and the excited state, respectively. When $S_i$ and $S_i^*$ are ordered antiferromagnetically, this external magnetic field brings about the so-called sublattice splitting of the exciton line as follows:

$$\Delta_i^{ex}=|2\delta_i^{ex}|\ , \tag{2}$$

where $\Delta_i^{ex}$ denotes the magnitude of the splitting.

The splitting of the $A0$ line with $\mathbf{H}_0\|\mathbf{a}$ shown in Figs. 1 and 2 is, then, the sublattice splitting. Thus, by substituting $\Delta_a^{ex}/H_0=3.86\times10^{-1}$ cm$^{-1}$kOe$^{-1}$ and $g_aS_a=4.25$ (Ref. 1) into Eqs. (1) and (2), we have

$$g_a^*S_a^*=0.116\ . \tag{3}$$

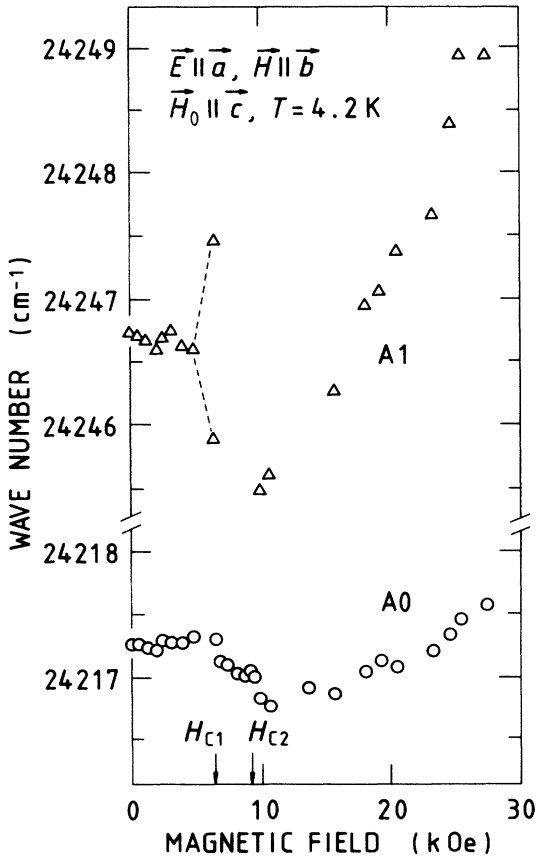


FIG. 3. Energy shifts of the $A0$ and $A1$ lines with $\mathbf{H}_0\|\mathbf{c}$ at 4.2 K. The dashed lines represent the splitting of the $A1$ line.

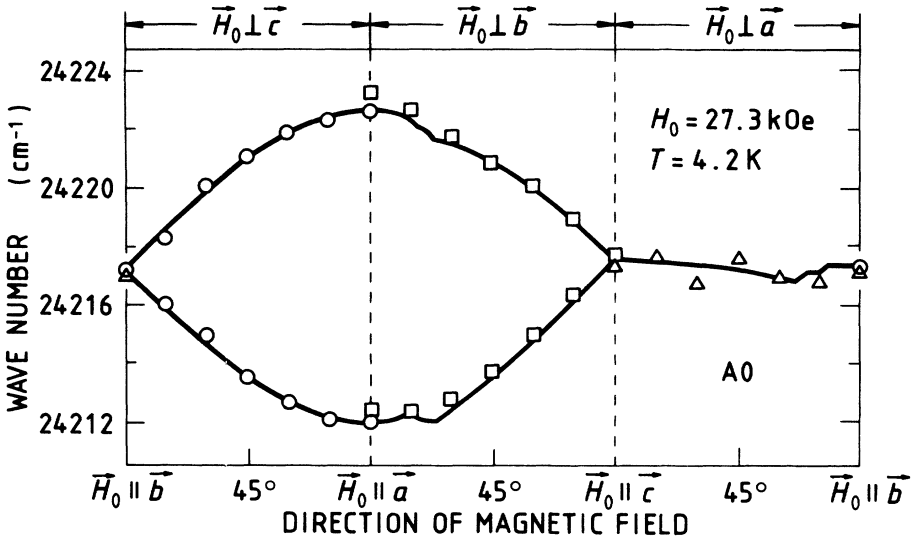


FIG. 4. Dependence of the energy shift of the $A0$ line on the direction of the external magnetic field (27.3 kOe). The symbols ○, □, and △ denote the results with the incident light parallel to the $c$ axis (**E**∥**a**,**H**∥**b**), the $b$ axis (**E**∥**a**,**H**∥**c**), and the $a$ axis (**E**∥**c**,**H**∥**b**), respectively. The solid curve is discussed in the text.

This value is much smaller than the magnetic moment of the ground state and can be neglected.

As shown in Fig. 3, the $A0$ line shifts monotonically with $\mathbf{H}_0 \| \mathbf{c}$ above 10 kOe, because all $S_c$ are ordered ferromagnetically in this magnetic field region. Thus, by substituting $\delta_c^{ex}/H_0 = 4.8 \times 10^{-2}$ $cm^{-1}kOe^{-1}$ and $g_c S_c = 1.14$ (Ref. 1) into Eq. (1), we have

$$g_c^* S_c^* = 0.112 \ . \tag{4}$$

This value is also negligible.

Under $\mathbf{H}_0 \| \mathbf{c}$ below 10 kOe, the sublattice splitting of the $A0$ line cannot be observed, for $\Delta_c^{ex}$ is very small. The steplike energy shifts at about 6.5 and 9.5 kOe are due to the metamagnetic transitions at $H_{c1}$ and $H_{c2}$, respectively. Since $g_c^* S_c^* \simeq 0$, the magnitude of the energy shift between zero field and $H_{c2}$ is expected to show only the magnitude of the interchain interactions $J_b + J_c$. In practice, the measured energy shift $-0.5$ $cm^{-1}$ is in fine agreement with $-0.49$ $cm^{-1}$, which is estimated from magnetization experiments.[1]

The $A0$ line does not vary with $\mathbf{H}_0 \| \mathbf{b}$. Then, we have

$$g_b^* S_b^* = 0 \ . \tag{5}$$

Now the experimental data mentioned up to this point indicate that the excited state corresponding to the $A0$ line has no magnetic moment. If this indication is true, the energy shift of the $A0$ line with external magnetic fields in all directions will be calculated only from $g_a S_a = 4.25$, $g_b S_b = 0$, $g_c S_c = 1.14$, and $J_b + J_c = -0.5$ $cm^{-1}$. The solid curve in Fig. 4 represents this calculation, where $\Delta_c^{ex}$ is neglected, and fits in the experimental result within the experimental errors. This fitness proves that the excited state corresponding to the $A0$ line has no magnetic moment in all directions. That is to say, this excited state is a singlet state.

### C. Assignment of the $A1$ line

The uniaxial stress effect on the $A1$ line is the same as that on the $A0$ line, and the intensity of the $A1$ line does not increase with temperature.[9] These data may suggest that the $A1$ line is the cold-magnon sideband of the exciton line $A0$.

Since $S_a$ are ordered antiferromagnetically along a chain, the energy shift of a magnon sideband with $\mathbf{H}_0 \| \mathbf{a}$, expressed by $\delta_a^{MS}$, is described as

$$\delta_a^{MS} = [g_a S_a - g_a^* S_a^* - g_a S_a + g_a (S-1)_a] \mu_B H_0 \ , \tag{6}$$

where $(S-1)$ represents one magnon creation. Furthermore, its sublattice splitting is evaluated by

$$\Delta_a^{MS} = |2\delta_a^{MS}| \ , \tag{7}$$

where $\Delta_a^{MS}$ denotes the magnitude of the splitting. By substituting $S = \frac{1}{2}$, $g_a S_a = 4.25$, and $g_a^* S_a^* \simeq 0$ into Eqs. (6) and (7), we obtain

$$\Delta_a^{MS}/H_0 \simeq 3.97 \times 10^{-1} \, cm^{-1} kOe^{-1} \ . \tag{8}$$

This magnitude is roughly equal to that of the splitting of the $A1$ line with $\mathbf{H}_0 \| \mathbf{a}$, $3.56 \times 10^{-1}$ $cm^{-1}kOe^{-1}$.

The energy shift of a magnon sideband with $\mathbf{H}_0 \| \mathbf{c}$ is different from that with $\mathbf{H}_0 \| \mathbf{a}$, because $S_c$ are ordered ferromagnetically along a chain even at zero magnetic field. Its energy shift with $\mathbf{H}_0 \| \mathbf{c}$ is calculated by

$$\delta_c^{MS} = [g_c S_c - g_c^* S_c^* + g_c S_c - g_c (S-1)_c] \mu_B H_0 \ . \tag{9}$$

Moreover, its sublattice splitting below $H_{c2}$ is calculated by

$$\Delta_c^{MS} = |2\delta_c^{MS}| \ . \tag{10}$$

Since $g_c S_c = -g_c (S-1)_c$ and $g_c^* S_c^* \simeq 0$, we get

$$\delta_c^{MS} \simeq 3\delta_c^{ex} \tag{11}$$

and

$$\Delta_c^{MS} \simeq 3\Delta_c^{ex} . \quad (12)$$

As can be seen from Fig. 3, the energy shift of the $A1$ line with $\mathbf{H}_0 \| \mathbf{c}$ is about three times larger than that of the $A0$ line, and the sublattice splitting of the $A1$ line is observed.

From the above consideration, we conclude the $A1$ line to be the cold-magnon sideband of the exciton line $A0$.

Now, the energy difference between the $A0$ and $A1$ lines is 29.5 $cm^{-1}$, which is almost half as large as the magnon excitation energy estimated from the exchange interaction ($2|J_a| = 56$ $cm^{-1}$). This reduction is interpreted as follows.

The magnon excitation energy of the $j$ site, $E_{mag}$, is given by

$$E_{mag} = 2|J_a|S_{j-1}(S-1)_j - 2|J_a|S_{j-1}S_j + 2|J_a|(S-1)_jS_{j+1} - 2|J_a|S_jS_{j+1} , \quad (13)$$

where the $(j-1)$ and $(j+1)$ sites are nearest-neighbor sites of the $j$ site within a chain. Put $S_{j-1}(S-1)_j = (S-1)_jS_{j+1} = \frac{1}{4}$ and $S_{j-1}S_j = S_jS_{j+1} = -\frac{1}{4}$; then

$$E_{mag} = 2|J_a| . \quad (14)$$

Besides, when an exciton is created on the $(j-1)$ site, the magnon excitation energy on the $J$ site, $E^*_{mag}$, is given by

$$E^*_{max} = 2|J_a^*|S^*_{j-1}(S-1)_j - 2|J_a^*|S^*_{j-1}S_j + 2|J_a|(S-1)_jS_{j+1} - 2|J_a|S_jS_{j+1} = 2|J_a^*|S^*_{j-1} + |J_a| , \quad (15)$$

where $J_a^*$ represents the exchange interaction between the ground and the excited state. Eventually, the energy difference between the exciton line and its magnon sideband is estimated at $E^*_{mag}$, not at $E_{mag}$. Since the energy difference between the $A0$ and $A1$ lines is nearly equal to $|J_a|$, the magnitude of $|J_a^*|S^*$ is nearly equal to zero. Accordingly, we determine that the exchange interaction between the ground and the excited state is very small. The smallness of this interaction is caused by the fact that the excited state is a singlet state, and this smallness makes an important contribution to the above-mentioned reduction in the energy difference between the $A0$ and $A1$ lines. Moreover, the one-dimensionality of the magnetic property also contributes to this reduction, because the magnon excitation energy is influenced by the states of neighbor sites almost only within a chain. The transition mechanism of the $A1$ line is illustrated in Fig. 5.

By the way, as shown in Fig. 1, the intensities of the two branches of the splitting $A1$ line under $\mathbf{H}_0 \| \mathbf{a}$ are different, and this difference increases as the higher-energy branch approaches the $A2$ line. This behavior is probably due to the mixing of the lowest and the second lowest excited state.

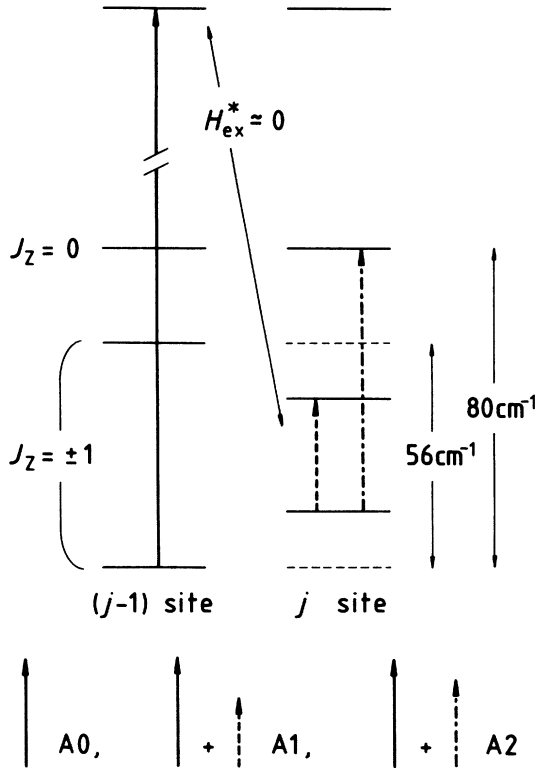


FIG. 5. Excitation schemes for the $A0$, $A1$, and $A2$ lines. The $(j-1)$ site is the nearest-neighbor site of the $j$ site within a chain. The symbol $J_z$ denotes the total angular momentum. The interaction between the ground and the excited state is expressed by $H^*_{ex}$, and the smallness of this interaction ($H^*_{ex} \simeq 0$) reduces the energy difference between the pseudodoublet ground state ($J_z = \pm 1$) on the $j$ site.

### D. Assignment of the $A2$ line

The uniaxial stress effect on the $A2$ line is the same as that on the $A0$ line, and the intensity of the $A2$ line does not increase with temperature.[9] These data may suggest that the $A2$ line is attributed to the simultaneous excitation of the $A0$ exciton and a spin flip. In addition, the $A2$ line scarcely varies with external magnetic fields in all directions. This result indicates that the above-mentioned spin flip corresponds to the electronic transition from the ground state to a singlet excited state at the nearest-neighbor site of the exciton creation. Consequently, we conclude the transition mechanism of the $A2$ line to be as in Fig. 5.

Taking account of the reduction of the magnon energy in the $A1$ line, we decide that the inherent energy difference between the ground state and this spin-flip excited state is larger than the energy difference between the $A0$ and $A2$ lines, 67.1 $cm^{-1}$. As can be seen from Fig. 5, the difference of this inherent energy from 67.1 $cm^{-1}$ is expected to have the half magnitude of the energy reduction in the $A1$ line. Consequently, this spin-flip excited state is estimated to lie about 80 $cm^{-1}$ higher than the ground state. By reference to the data of Mössbauer and heat capacity experiments,[2,10] we con-

clude this excited state to be the second lowest excited state of the $Fe^{2+}$ ground multipet $^5T_2(D)$.

## IV. SPECTRA AROUND THE NÉEL TEMPERATURE

### A. Experimental results

Here, we summarize the important temperature variation of the above-mentioned fine structure without external magnetic field.[9] Below about 10 K, the fine structure scarcely varies with the rise of temperature. Above about 10 K, the extra absorption lines $H1$ and $H3$ are observed about 33 $cm^{-1}$ higher and about 29 $cm^{-1}$ lower than the $A0$ line, respectively. The $A1$ line cannot be observed above about 20 K owing to the $H1$ line. The $H1$ line has not been assigned. The $H3$ line is assigned to the $A0$ exciton creation at a thermally excited magnetic domain-wall site.

Now, the fine structure varies remarkably with $\mathbf{H}_0\|\mathbf{a}$ also around $T_N$. Figure 6 shows this variation at 12.9 K in $\mathbf{E}\|\mathbf{a}$. The $H3$ line splits into two branches, and the energy difference between them is $3.5\times10^{-1}$ $cm^{-1}kOe^{-1}$. The other absorption lines also split into two branches. Figure 7 shows the temperature variation of the fine structure in $\mathbf{E}\|\mathbf{a}$ under $\mathbf{H}_0$(28.7 kOe)$\|\mathbf{a}$. The intensities of the two branches of the splitting $H3$ line are different, and this difference decreases with the rise of temperature. This behavior is shown in Fig. 8.

### B. Thermally excited magnetic domain wall

The $H3$ line splits into two branches with $\mathbf{H}_0\|\mathbf{a}$, and the energy difference between them is $3.5\times10^{-1}$ $cm^{-1}kOe^{-1}$. This value is almost constant from 11 to 18 K and roughly equals $2g_aS_a\mu_B$, $3.97\times10^{-1}$ $cm^{-1}kOe^{-1}$, within the experimental errors. The intensities of the two

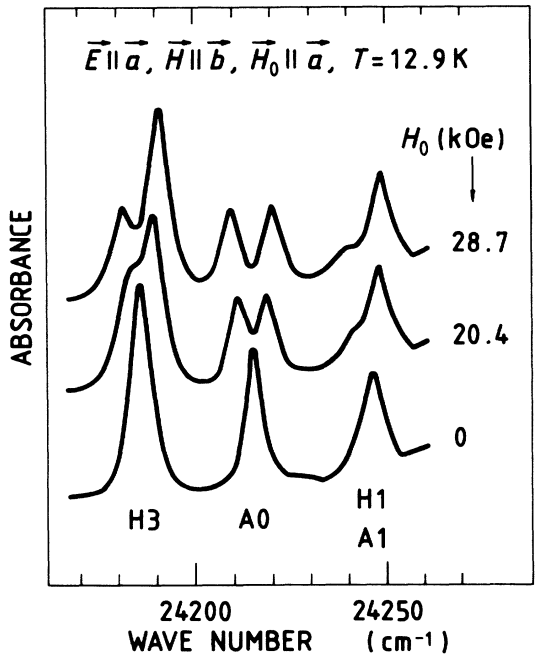


FIG. 6. Variation of the absorption spectra with $\mathbf{H}_0\|\mathbf{a}$ at 12.9 K. The $A1$ and $H1$ lines overlap each other near 24 250 $cm^{-1}$.

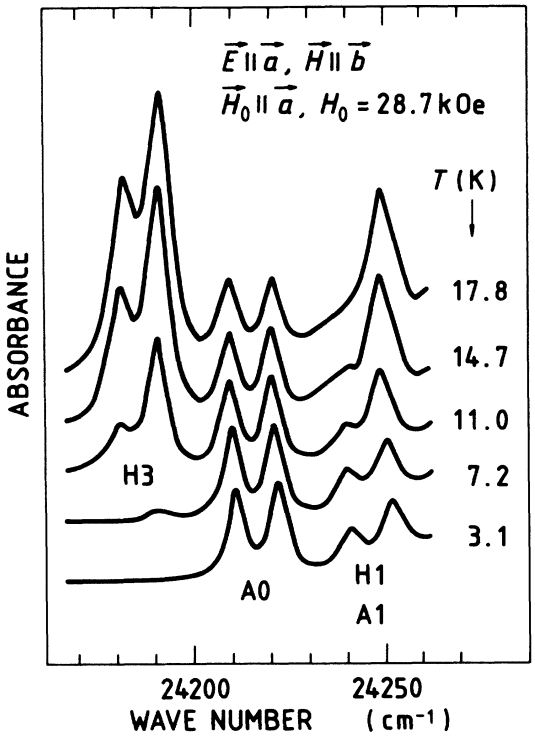


FIG. 7. Temperature variation of the absorption spectra under $\mathbf{H}_0$(28.7 kOe)$\|\mathbf{a}$. The $A1$ and $H1$ lines overlap each other near 24 250 $cm^{-1}$.

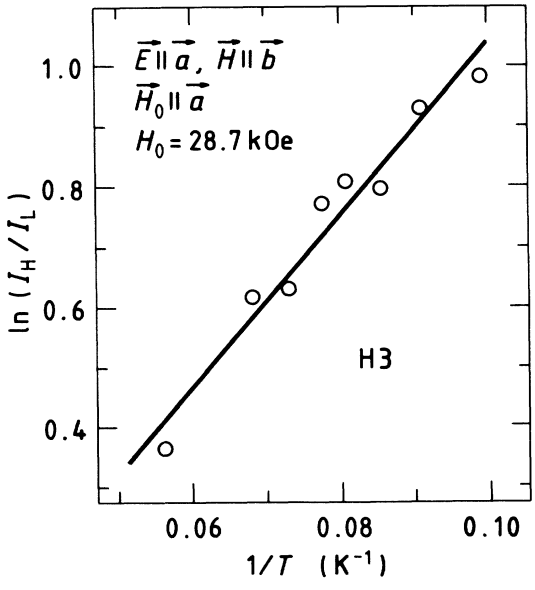


FIG. 8. The temperature dependence of the intensity difference between two branches of the splitting $H3$ line under $\mathbf{H}_0$(28.7 kOe)$\|\mathbf{a}$. The symbols $I_H$ and $I_L$ denote the integrated intensities of the higher- and lower-energy branch, respectively. The solid line is computed using a least-squares program and represents $I_H/I_L = \exp[(14.2/T) - 0.386]$.

branches are different, as can be seen from the solid line in Fig. 8, this intensity difference under $\mathbf{H}_0(28.7\ \text{kOe})\|\mathbf{a}$ varies in accordance with

$$I_H/I_L=\exp[(14.2/T)-0.386], \quad (16)$$

where $I_H$ and $I_L$ denote the integrated intensities of the higher- and lower-energy branch, respectively. The parameter 14.2 K (9.9 $\text{cm}^{-1}$) is almost equal to the magnitude of the splitting, about 10 $\text{cm}^{-1}$. We interpret these features of the $H3$ line as follows.

Under $\mathbf{H}_0\|\mathbf{a}$, thermally excited magnetic domain walls can be classified into two groups by the difference in the direction of their $S_a$. In other words, their $S_a$ have the same or the opposite direction of $\mathbf{H}_0$. The energy difference between these two groups is estimated at $2g_aS_a\mu_B\mathbf{H}_0$. This energy difference is considered to be the only occasion of the splitting of the $H3$ line, because the excited state corresponding to the $H3$ line is a singlet state. In addition, the thermal populations of these two groups are different, and this population difference is estimated to be $\exp(2g_aS_a\mu_BH_0/kT)$. As mentioned above, the intensity difference between the two branches of the splitting $H3$ line varies with temperature agreeably to such an exponential law. Consequently, we conclude that this intensity difference is caused by the population difference between the two groups of the domain walls. However, the extra constant in Eq. (16), $-0.386$, cannot have been explained.

By the above consideration, the higher-energy branch of the splitting $H3$ line under $\mathbf{H}_0\|\mathbf{a}$ is assigned to the $A0$ exciton creation at a thermally excited domain-wall site of which $S_a$ has the opposite direction of $\mathbf{H}_0$. On the other hand, the domain-wall site associated with the lower-energy branch has $S_a$, of which the direction is the same as $\mathbf{H}_0$.

### C. Domain wall induced by external magnetic field

The domain walls associated with the $H3$ line are thermally excited ones. Besides such a case, when the transition between the antiferromagnetic and the ferromagnetic phase occurs with an external magnetic field, this field is able to induce domain walls, e.g., $\cdots\downarrow\uparrow\downarrow\uparrow\uparrow\uparrow\uparrow\cdots$.

As regards the above, the following experimental result has been obtained in Ref. 8. With $\mathbf{H}_0\|\mathbf{a}$, such a phase transition occurs gradually in the 120–160-kOe region at 4.2 K; simultaneously, the extra absorption line $A0'$ observed near 24 220 $\text{cm}^{-1}$, and the field dependence of its intensity indicates that this absorption line is associated with the domain walls induced by the field.

If the $A0'$ line is assigned to the $A0$ excitation creation at such a domain-wall site of which $S_a$ has the opposite direction of $H_0$, its peak energy will fit in with the extrapolation of the energy shift of the higher-energy branch of the splitting $H3$ line with $\mathbf{H}_0\|\mathbf{a}$. In fact, as can be seen from Fig. 9, this fitness is very good. Therefore, it is concluded that the $A0'$ line is assigned to the $A0$ exciton creation at a domain-wall site that is induced by $\mathbf{H}_0\|\mathbf{a}$.

On the other hand, as mentioned in Sec. I, two

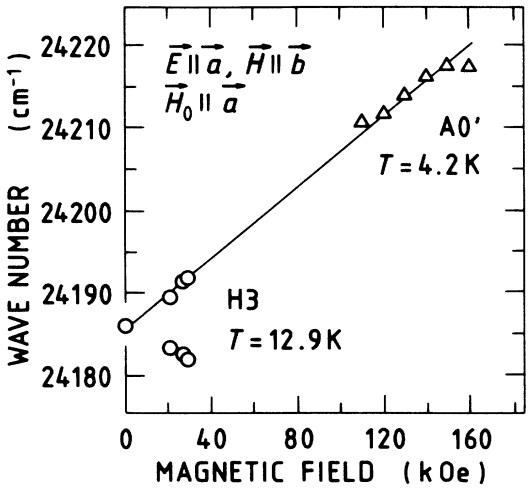


FIG. 9. Energy shifts of the $H3$ line and the $A0'$ line (from Ref. 8) with $\mathbf{H}_0\|\mathbf{a}$. The solid line is to guide the reader's eye.

metamagnetic phase transitions occur at $H_{c1}$ (6.5 kOe) and $H_{c2}$ (9.5 kOe) at 4.2 K.[-1] This data may suggest that $\mathbf{H}_0\|\mathbf{c}$ is also able to induce the domain walls. Nevertheless, in the present experiment, no extra absorption line is observed under $\mathbf{H}_0\|\mathbf{c}$ at 4.2 K. From this result, we draw the conclusion that $\mathbf{H}_0\|\mathbf{c}$ induces no domain wall within a chain. That is to say, spins within a chain reverse alto-

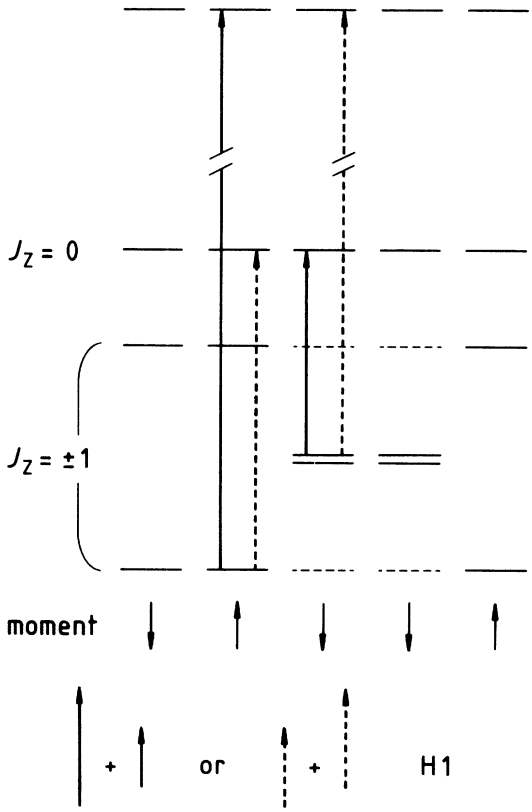


FIG. 10. Excitation schemes for the $H1$ line. There are two possible schemes, the solid and the dashed arrows. The energy reduction between the pseudodoublet ground state ($J_z=\pm1$), shown in Fig. 5, is neglected in this figure.

gether with $\mathbf{H}_0 \| \mathbf{c}$. By the way, a detailed magnetization experiment[7] has shown these metamagnetic transitions to occur noncritically below 2 K. However, at 1.7 K, no extra absorption line is observed under $\mathbf{H}_0 \| \mathbf{c}$ either. Thus, $\mathbf{H}_0 \| \mathbf{c}$ is concluded not to induce domain walls within a chain even below 2 K. Then, within a single chain, the direction of every $S_c$ is the same as every other. The noncriticality of these transitions below 2 K is probably occasioned by the coexistence of the two types of the chains, of which $S_c$ have the same or the opposite direction of $\mathbf{H}_0 \| \mathbf{c}$.

### D. Assignment of the $H1$ line

The $H1$ line is observed above about 10 K at zero magnetic field,[9] so this absorption line is probably associated with thermally excited domain walls.

Figure 7 shows the temperature variation of the spectra under $\mathbf{H}_0(28.7\ \text{kOe}) \| \mathbf{a}$, and the $H1$ and $A1$ lines cannot be resolved into each line. However, we believe the $H1$ line to be much more dominant than the $A1$ line at 17.8 K, because, as can be seen from the large intensity of the $H3$ line, many domain walls are thermally excited at this temperature under $\mathbf{H}_0(28.7\ \text{kOe}) \| \mathbf{a}$. Accordingly, the $H1$ line does not split with $\mathbf{H}_0 \| \mathbf{a}$. By these data and the peak energy of the $H1$ line, we attribute the $H1$ line to the $A2$-like transition at a domain-wall site (see Fig. 10).

## V. CONCLUSION

The $A1$ line is the cold-magnon sideband of the exciton line $A0$. The $A2$ line is assigned to the cooperative excitation of the $A0$ exciton and the electronic transition from the ground state to the second lowest excited state of the $Fe^{2+}$ ground multiplet. The $H1$ line is assigned to the $A2$-like transition at a thermally excited domain-wall site.

The magnetic field dependence of the $A0$ line proves that the excited state corresponding to this absorption line is a singlet state. Since this excited state has no magnetic moment, the exchange interaction between the ground and this excited state is expected to be very little. The smallness of this interaction and the one-dimensionality of the magnetic property are the cause that the energy difference between the exciton line $A0$ and its magnon sideband $A1$ is almost 50% smaller than the magnon excitation energy.

From the energy shift of the $A0$ line with $\mathbf{H}_0 \| \mathbf{c}$, the interchain interactions are estimated to be $J_b + J_c = -0.5\ \text{cm}^{-1}$.

TABLE I. Assignments of absorption lines.

| Label | Initial state | | Final state |
|---|---|---|---|
| $A0$ | $\cdots\downarrow\uparrow\downarrow\uparrow\downarrow\uparrow\downarrow\cdots$ | [a]→ | $\cdots\downarrow\uparrow\downarrow*\downarrow\uparrow\downarrow\cdots$ [b] |
| $A1$ | $\cdots\downarrow\uparrow\downarrow\uparrow\downarrow\uparrow\downarrow\cdots$ | [a]→ | $\cdots\downarrow\uparrow\downarrow*\uparrow\uparrow\downarrow\cdots$ |
| $A2$ | $\cdots\downarrow\uparrow\downarrow\uparrow\downarrow\uparrow\downarrow\cdots$ | [a]→ | $\cdots\downarrow\uparrow\downarrow*0\uparrow\downarrow\cdots$ [c] |
| $H1$ [d] | $\cdots\downarrow\uparrow\downarrow\uparrow\downarrow\uparrow\uparrow\cdots$ | [e]→ | $\cdots\downarrow\uparrow\downarrow*0\downarrow\uparrow\cdots$ |
| | $\cdots\downarrow\uparrow\downarrow\uparrow\downarrow\uparrow\uparrow\cdots$ | [e]→ | $\cdots\downarrow\uparrow\downarrow0*\downarrow\uparrow\cdots$ |
| $H2$ | $\cdots\downarrow\uparrow\downarrow0\downarrow\uparrow\downarrow\cdots$ | [f]→ | $\cdots\downarrow\uparrow\downarrow0*\uparrow\downarrow\cdots$ |
| $H3$ | $\cdots\downarrow\uparrow\downarrow\uparrow\downarrow\uparrow\uparrow\cdots$ | [e]→ | $\cdots\downarrow\uparrow\downarrow*\uparrow\downarrow\uparrow\cdots$ |
| $H4$ | $\cdots\downarrow\uparrow\downarrow0\downarrow\uparrow\downarrow\cdots$ | [f]→ | $\cdots\downarrow\uparrow\downarrow*\downarrow\uparrow\downarrow\cdots$ |
| $A0'$ [g] | $\cdots\downarrow\uparrow\downarrow\uparrow\uparrow\uparrow\uparrow\cdots$ | [h]→ | $\cdots\downarrow\uparrow\downarrow*\uparrow\uparrow\uparrow\cdots$ |

[a] The Néel state.
[b] The symbol * represents an exciton creation site.
[c] The symbol 0 represents the singlet-state site, which is the second lowest excited-state site.
[d] There are two possible assignments of the $H1$ line.
[e] A thermally excited domain-wall state.
[f] A thermally excited singlet state.
[g] See Sec. IV C and Ref. 8.
[h] A domain-wall state induced by the $\mathbf{H}_0 \| \mathbf{a}$ axis.

The $H3$ line, which is ascribed to the $A0$ exciton creation at a thermally excited domain-wall site, splits into two branches with $\mathbf{H}_0 \| \mathbf{a}$, and their intensities are different. The cause of this splitting and intensity difference is the coexistence of the two groups of the domain walls, of which $S_a$ has the same or opposite direction of $\mathbf{H}_0 \| \mathbf{a}$.

Under $\mathbf{H}_0 \| \mathbf{a}$, the extra absorption line $A0'$ has been observed in the 120–160-kOe region at 4.2 K.[8] Its peak energy closely fits in with the extrapolation of the energy shift of the higher-energy branch of the splitting $H3$ line with $\mathbf{H}_0 \| \mathbf{a}$ around $T_N$. This fitness shows that this extra absorption line $A0'$ is assigned to the $A0$ exciton creation at a domain-wall site induced by $\mathbf{H}_0 \| \mathbf{a}$ (from 120 to 160 kOe). On the other hand, no domain wall is induced within a chain by $\mathbf{H}_0 \| \mathbf{c}$ because spins within a chain reverse all together with $\mathbf{H}_0 \| \mathbf{c}$.

The assignments of the absorption lines described in the present and the preceding paper are summarized in Table I.

## ACKNOWLEDGMENTS

H. O. wishes to thank Dr. I. Mogi of Tohoku University for his helpful advice. Moreover, the author gratefully acknowledges valuable discussions with Professor T. Murao of the University of Osaka Prefecture.

[1] J. A. J. Basten, Q. A. G. van Vlimmeren, and W. J. M. de Jonge, Phys. Rev. B **18**, 2179 (1978).
[2] H. Th. Le Fever, R. C. Thiel, W. J. Huiskamp, and W. J. M. de Jonge, Physica (Utrecht) **111B**, 190 (1981); H. Th. Le Fever, R. C. Thiel, W. J. Huiskamp, W. J. M. de Jonge, and A. M. van der Kraan, *ibid.* **111B**, 209 (1981).
[3] R. C. Thiel, H. de Graaf, and L. J. de Jongh, Phys. Rev. Lett. **47**, 1415 (1981).
[4] A. M. C. Tinus, C. J. M. Denissen, H. Nishihara, and W. J. M. de Jonge, J. Phys. C **15**, L791 (1982).
[5] J. P. M. Smeets, K. M. H. Maessen, E. Frikkee, and K. Kopinga, J. Magn. Magn. Mater. **31-34**, 1163 (1983).

[6]K. Kopinga, M. Steiner, and W. J. M. de Jonge, J. Phys. C **18**, 3511 (1985).
[7]J. P. M. Smeets, E. Frikee, W. J. M. de Jonge, and K. Kopinga, Phys. Rev. B **31**, 7323 (1985).
[8]M. Takeda, G. Kido, I. Mogi, Y. Nakagawa, H. Okada, and N. Kojima, J. Phys. Soc. Jpn. **58**, 3418 (1989).
[9]H. Okada, N. Kojima, T. Ban, and I. Tsujikawa, preceding paper, Phys. Rev. B **42**, 11 610 (1990).
[10]K. Kopinga, Q. A. G. van Vlimmeren, A. L. M. Bongaarts, and W. J. M. de Jonge, Physica (Utrecht) **86-88B**, 671 (1977).